PL-TR-92-2251

AD-A261 725

MULTIVARIATE SEISMIC CALIBRATION FOR THE NOVAYA ZEMLYA TEST SITE

DTIC
S ELECTE **D**
FEB 2 5 1993
C

Mark D. Fisk
Ralph W. Alewine, III
Henry L. Gray
Gary D. McCartor

Mission Research Corporation
P.O. Drawer 719
Santa Barbara, CA 93102-0719

30 September 1992

Scientific Report No. 2

93-03947

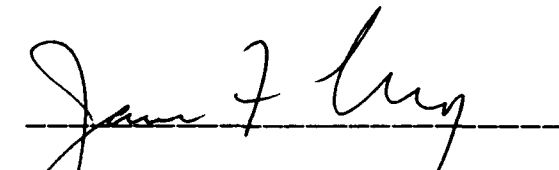Approved for public release; distribution unlimited

PHILLIPS LABORATORY
Directorate of Geophysics
AIR FORCE MATERIEL COMMAND
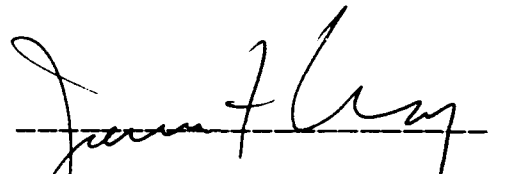**HANSCOM AIR FORCE BASE, MA 01731-5000**

93 2 24 056

The views and conclusions contained in this document are those of the authors and should not be interpreted as representing the official policies, either expressed or implied, of the Air Force or the U.S. Government.

This technical report has been reviewed and is approved for publication.

JAMES F. LEWKOWICZ
Solid Earth Geophysics Branch
Earth Sciences Division

JAMES F. LEWKOWICZ
Solid Earth Geophysics Branch
Earth Sciences Division

DONALD H. ECKHARDT, Director
Earth Sciences Division

This document has been reviewed by the ESD Public Affairs Office (PA) and is releasable to the National Technical Information Service (NTIS).

Qualified requestors may obtain additional copies from the Defense Technical Information Center. All others should apply to the National Technical Information Service.

If your address has changed, or if you wish to be removed from the mailing list, or if the addressee is no longer employed by your organization, please notify PL/IMA, Hanscom AFB MA 01731-5000. This will assist us in maintaining a current mailing list.

Do not return copies of this report unless contractual obligations or notices on a specific document requires that it be returned.

REPORT DOCUMENTATION PAGE

Public reporting burden for this collection of Information is estimated to average 1 hour per response, Including the time for reviewing Instructions, searching existing data sources, gathering and maintaining the data needed, and completing and reviewing the collection of Information. Send comments regarding this burden estimate or any other aspect of the collection of Information, Including suggestions for reducing this burden, to Washington Headquarters Services, Directorate for Information Operations and Reports, 1215 Jefferson Davis Highway, Suite 1204, Arlington, VA 22202-4302, and to the Office of Management and Budget, Paperwork Reduction Project (0704-0188), Washington, DC 20503.

1. AGENCY USE ONLY *(Leave blank)*	2. REPORT DATE 920930	3. REPORT TYPE AND DATES COVERED Scientific No. 2 910627 to 920622

4. TITLE AND SUBTITLE
MULTIVARIATE SEISMIC CALIBRATION FOR
THE NOVAYA ZEMLYA TEST SITE

5. FUNDING NUMBERS
PE62714E
PR9A10 TADA WUAC
Contract F19628-90-C-0135

6. AUTHOR(s)
Mark D. Fisk   Ralph W. Alewine, III*
Henry L. Gray**   Gary D. McCartor**

7. PERFORMING ORGANIZATION NAME(S) AND ADDRESS(ES)
Mission Research Corporation
P.O. Drawer 719
Santa Barbara, CA 93102-0719

8. PERFORMING ORGANIZATION REPORT NUMBER
MRC-R-1402

9. SPONSORING/MONITORING AGENCY NAME(S) AND ADDRESS(ES)
Phillips Laboratory
Hanscom Air Force Base
Massachusetts 01731-5000
Attn: James Lewkowicz/GPEH

10. SPONSORING/MONITORING AGENCY REPORT NUMBER
PL-TR-92-2251

11. SUPPLEMENTARY NOTES
* DARPA/NMRO
** Southern Methodist University, Dallas, TX

12a. DISTRIBUTION/AVAILABILITY STATEMENT

Approved for public release; distribution unlimited

12b. DISTRIBUTION CODE

13. ABSTRACT *(Maximum 200 words)*

Within the last year, Soviet yield data have been acquired by DARPA for over 40 underground nuclear explosions at the Novaya Zemlya Test Site between 1964 and 1990. These yields are compared to previous estimates by other authors, based on observed seismic magnitudes and magnitude–log yield relations transported from other test sites. Several discrepancies in the yield data are noted. Seismic magnitude data, based on NORSAR Lg and P coda, Gräfenberg Lg, and a world-wide m_b, have been published by Ringdal and Fyen (1991) for 18 of these events. A similar set of Soviet network magnitudes have been published by Israelsson (1992). Using these data, estimates of the multivariate calibration parameters of the magnitude-log yield relations are computed. An outlier test is applied to the the residuals to the lines of best fit. One of the two smallest events is identified as an outlier for every multivariate magnitude combination. A classical confidence interval is presented to estimate future yields, based on estimates of the unknown multivariate calibration parameters. A test of TTBT compliance and a definition of the F-number, based on the confidence interval, are also provided. F-number estimates are obtained for various magnitude combinations by jackknifing. The reliability of the results is discussed, in light of the fact that the data are tightly clustered for 16 of the 18 events.

14. SUBJECT TERMS Multivariate calibration Novaya Zemlya Test Site yield estimation NORSAR confidence intervals Graefenberg	15. NUMBER OF PAGES 50
	16. PRICE CODE

17. Security CLASSIFICATION OF REPORT UNCLASSIFIED	18. Security CLASSIFICATION OF THIS PAGE UNCLASSIFIED	19. Security CLASSIFICATION OF ABSTRACT UNCLASSIFIED	20. LIMITATION OF ABSTRACT SAR

TABLE OF CONTENTS

LIST OF ILLUSTRATIONS

LIST OF TABLES

SECTION 1

INTRODUCTION

Seismic calibration and yield estimation for the Novaya Zemlya test site (NZ) are still matters of some interest and continued research; if underground nuclear testing resumes in the former Soviet Union, it is likely to be at the northern Novaya Zemlya site (NNZ). (No tests have been performed at the southern site (SNZ) since 1975, e.g., Lay, 1991.) Accurate magnitude–log yield calibration for NNZ has been hindered in the past by the lack of yield information to accompany a wide variety of published seismic magnitude data. Recently, yield data for 42 underground nuclear tests conducted at NZ have been provided to DARPA by an official of the former Soviet Union. The focus of this report is on comparing these yields with previous estimates and on computing estimates of the multivariate magnitude–log yield calibration parameters.

Teleseismic body wave magnitudes, m_b, have been given by the International Seismic Centre (ISC), Sykes and Ruggi (1988), Burger et al. (1986), and Chan et al. (1988b). Nuttli (1988) and Sykes and Ruggi (1988) provide sets of $m_b(Lg)$ and M_S magnitudes, respectively. Chan et al. (1988a,b) and Lilwall and Marshall (1986) give magnitudes based on P and P'P'. These data and yield estimates based on these data and others are reviewed by Lay (1991). More recently, Ringdal and Fyen (1991) have published world-wide m_b values, RMS Lg and P coda values recorded at NORSAR, and RMS Lg values recorded at Gräfenberg for 18 events at NNZ between 29 September 1976 and 24 October 1990. Israelsson (1992) has published a set of Soviet network magnitudes based on RMS amplitudes in time windows corresponding to initial P, P coda, S with coda, and Lg for 17 of the same 18 events.

Epicentral locations of many of the tests were determined by Lilwall and Marshall (1986). Others were determined at the Center for Seismic Studies (CSS) and the ISC. Israelsson (1992) provides a review of the epicentral locations of 21 of the tests at NNZ. Due to the complicated topography of the northern site, these tests were mainly emplaced in near-horizontal tunnels in the mountains. Leith et al. (1990) and Lay (1991) provide reviews of the test site geology, topography, tectonic release and complex surface interactions and propagation effects.

The Soviet yield data used in our study was presented by Victor Mikhailov of the former Soviet Union at a meeting in Norway in September 1991. Several apparent discrepancies in the data were pointed out to us by Richards (1992). More

1

recent discussions with Aduṣhkin et al. (1992) at the 14th Annual PL/DARPA Seismic Research Symposium in Tucson have resolved some of the discrepancies. However, they brought into question the accuracy of the data. Thus, the magnitude–log yield results presented here are preliminary and contingent on the accuracy of the yield data.

The remainder of this report is organized as follows. In Section 2 we present the Soviet yield data and compare it to previous yield estimates based on observed seismic magnitudes and magnitude–log yield relations transported from other sites. We discuss the discrepancies associated with the yield data. In Section 2 we also provide the magnitude data, used in our analysis (from Ringdal and Fyen, 1991, and Israelsson, 1992).

In Section 3 we provide the statistical background needed for this study. In Section 3.1 we present multivariate regression analysis and in Section 3.2 we present a 95% confidence interval for the yield of a new event. The confidence interval is based on multivariate data and the treatment of all model parameters as unknown. It was originally derived by Brown (1982) and has been used previously by Shumway and Der (1990) to compute yield intervals for Semipalatinsk explosions. We also describe how TTBT compliance may be tested and define the F-number in terms of the confidence interval. In Section 3.3 we present an outlier test, which we later apply to the data.

In Section 4 we provide the results of calibration, outlier, and yield estimation for the magnitude data from Ringdal and Fyen (1991). In Section 4.1 we provide estimates of the calibration parameters, including the random error correlation coefficients. In Section 4.2 we discuss which events have residuals that are identified as outliers. In Section 4.3 we provide estimates of the F-number means and standard deviations for various magnitude combinations, obtained by jackknifing. In Section 5 we repeat this analysis for the Soviet network magnitudes for Israelsson (1992). Last, in Section 6 we provide some concluding remarks and a review the best calibration parameter estimates.

SECTION 2

DATA

2.1 Novaya Zemlya Yield Data.

Within the last year, yield data for 42 underground nuclear tests conducted at NZ were provided to DARPA by an official of the former Soviet Union. The original bar graph of the yield data is shown in Figure 1. The year and number of events tested in that year (in parentheses) are labeled along the x-axis, and the month and accumulated number of events tested during a particular month are labeled along the left and right edges of the y-axis, respectively. The dates of each event are listed at the top of the graph. We have determined the yields by digitizing the bar lengths and comparing them to the length of the 150 KT scale at the left edge of the graph.

Table 1 lists the dates provided with the original data, our determination of the yields, Y(FGM), as well as previous estimates of some of the yields by Nuttli (1988), Y(Nuttli), Sykes and Ruggi (1988), Y(SR), and Burger et al. (1986), Y(BBL). The yield estimates by Nuttli (1988) were based on a quadratic fit of Lg magnitudes to the log yields of NTS events. The fit was then transported to NZ with no corrections. The yields from Sykes and Ruggi (1988) were estimated from a linear regression model for m_b, assuming bias corrections relative to NTS and Amchitka. The yields from Burger et al. (1986) were estimated by scaling relative to an Amchitka event. These and other yield estimates of NZ events have been compiled previously by Lay (1991); we present them here for comparison. Jih and Wagner (1992) have also estimated the yields of 28 of these events based on path corrected short-period teleseismic P-wave amplitudes and experience at Semipalatinsk and NTS.

There are several points regarding the new yield set that should be noted. First, there are breaks in 7 of the 8 longest bars. These events are larger that 1 MT, as confirmed by the yield estimates, but the bars do not provide accurate measures of the yields. Second, our estimates of the very small events (12, 20, 21, 37) have limited accuracy; in fact, we do not currently know the accuracy with which any of the yields were recorded on this graph. Third, the graph in Figure 1 shows a small event on 27 July 1972, which is not present in any of the other data sets we have examined. We have learned from Richards (1992) that this test may have never occurred. Adushkin et al. (1992) have confirmed that this test did not occur.

3

Рис.2   Хроника подземных ядерных испытаний на Северном полигоне (1964 - 1990 г.г.)
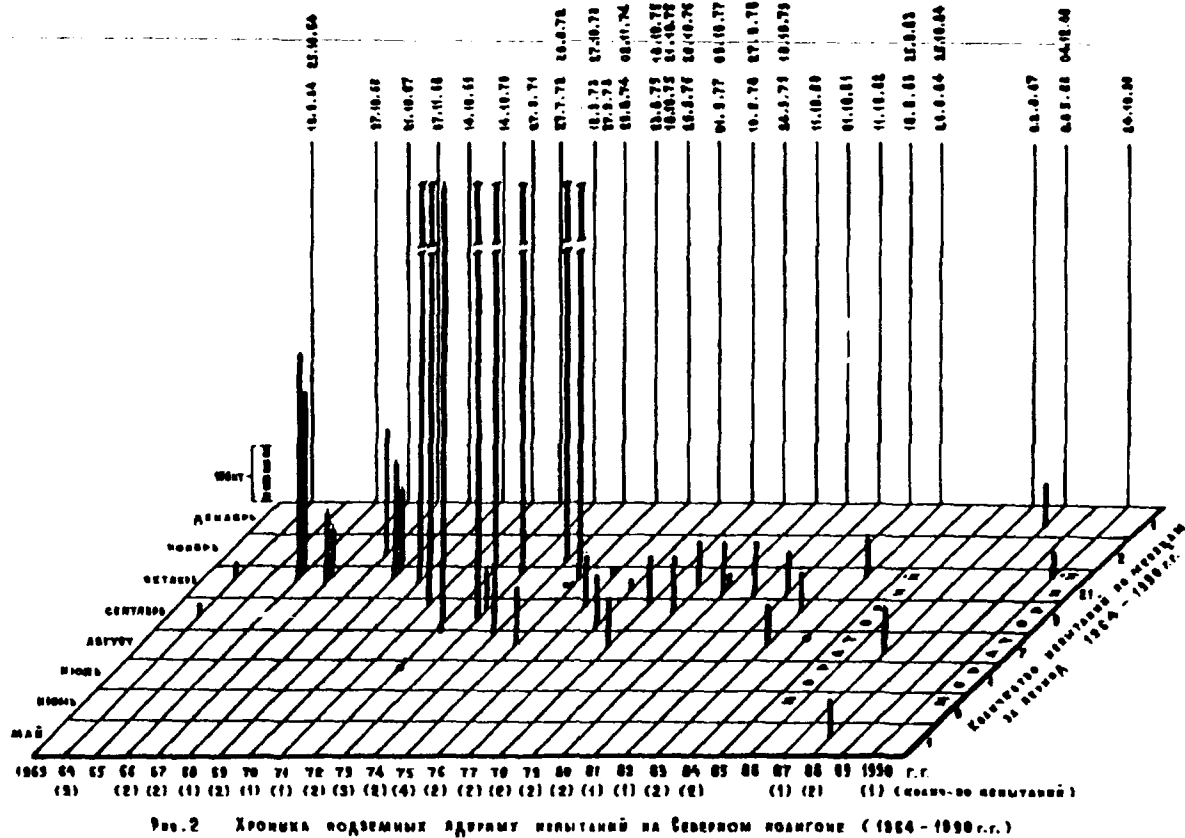
Figure 1.   Original bar graph of Soviet yield data for 42 underground nuclear tests conducted at Novaya Zemlya.

Fourth, the two events on 18 October 1975 are known to be double explosions at SNZ (Hurley, 1977; Subhash and Choudhury, 1979; Burger et al., 1986, Chan et al., 1988a), and all available yield estimates suggest that these were large events, on the order of a megaton or more. These events are, however, characterized as very small on the bar graph (Figure 1). This discrepancy was first pointed out to us by Richards (1992). Adushkin et al. (1992) have confirmed that the yields were, in fact, on the order of a megaton or more.

Fifth, Lilwall and Marshall (1986) and Stewart and Marshall (1988) suggested that the event on 11 October 1980 was also a double explosion, with shots separated by approximately 7 km. They determined that the ratio of the yields was roughly a factor of 0.35. This is consistent with our yield determinations given in Table 1, Y(FGM), for these events.

4

Table 1. Yield determinations and estimates of Novaya Zemlya tests.

Event	Date	Y (FGM)	Y (Nuttli)	Y (SR)	Y (BBL)
1	640918	29	2.5	2	---
2	641025	40	16.4	8	---
3	661027	603	644	422	600
4	661027	485	---	---	---
5	671021	184	180	93	61
6	671021	126	---	---	---
7	681107	334	253	119	110
8	691014	302	399	140	183
9	691014	219	---	---	---
10	701014	>1000	1970	1001	1714
11	710927	>1000	1500	586	973
12	720727	14	---	---	---
13	720828	1183	580	329	426
14	730912	>1000	3510	2099	2824
15	730927	102	129	100	36
16	731027	>1000	4990	4055	3886
17	740829	>1000	1110	497	629
18	741102	>1000	2840	2099	1624
19	750823	152	690	477	604
20	751018	10	2220	1281	1166
21	751018	10	---	---	---
22	751021	>1000	600	497	554
23	760929	131	91	70	---
24	761020	22	19	13	---
25	770901	134	122	55	---
26	771009	27	10	4	---
27	780810	121	91	89	---
28	780927	125	61	44	---
29	790924	144	81	55	---
30	791018	120	79	70	---
31	801011	139	76	55	---
32	801011	30	---	---	---
33	811001	136	116	113	---
34	821011	107	79	44	---
35	830818	105	145	89	---
36	830925	97	99	70	---
37	840826	10	---	---	---
38	841025	101	---	89	---
39	870802	121	---	70	---
40	880507	97	---	---	---
41	881204	112	---	---	---
42	901024	64	---	---	---

5

Last, many of the yields are consistent with previous estimates; however, there are several events for which the yields differ significantly. Adushkin et al. (1992) suggested that the accuracy of the bar graph in Figure 1 is questionable. Clearly, the accuracy of these yield data needs to be resolved, and we are pursuing this matter currently. Hence, although there are no known discrepancies associated with the events used to obtain the calibration results, given below, our results are preliminary and contingent on the accuracy of the original yield data.

2.2 Magnitude Data.

Ringdal and Fyen (1991) have published a set of magnitudes, based on NORSAR Lg and P coda, Gräfenberg Lg, and a world-wide m_b, for 18 underground nuclear tests conducted between 29 September 1976 and 24 October 1990 at NNZ. (See Ringdal and Fyen, 1991, and references therein for descriptions of the arrays and the methods used to compute the magnitudes.) Table 2 lists the event numbers, dates, yields and magnitudes of those tests. Low SNR at Gräfenberg for event 26 did not allow for a reliable RMS Lg determination. Also, no NORSAR data are available for event 28, and event 37 was too small to provide reliable magnitude determinations from either array. The magnitudes corresponding to the double explosion on 11 October 1980 (events 31 and 32) may be biased from interference effects. We have associated the magnitudes with the larger of the two yields; using the root sum of the squares of the combined yields (142 KT) produces an insignificant change in the results.

Israelsson (1992) has published a set of Soviet network magnitudes, which we will also consider in our study. The network is comprised of nine stations, Apatity (APA), Arti (ARU), Bodaybo (BOD), Chusal (CHS), Norilsk (NRI), Novosibirsk (NVS), Obninsk (OBN), Talaya (TLY), and Uzhgorod (UZH). (See Israelsson, 1992, for the locations of these stations, a description of the seismometers, and further details on the results.) Analog recordings of 111 waveforms for 21 explosions from the nine stations were hand-digitized. Although his study emphasized RMS Lg in the group velocity window between 3.1–3.7 km/s, he also computed RMS amplitudes corresponding to initial P in the time window from onset to 20 s after onset, P coda in the time window 20 s after onset to 15 s before the expected S arrival, and S with coda in the time window 15 s prior to the expected S arrival to a group velocity of 3.7 km/s.

RMS amplitudes, computed from bandpass filtered traces, were corrected for noise and normalized to the OBN instrument. Station magnitudes were obtained by taking the logarithm, and then shifted by a constant, for each station and phase,

6

Table 2.   Magnitude data from Ringdal and Fyen (1991) for 18 tests at NNZ.

Event	Date	Y (kt)	NAO Lg	GRF Lg	NAO P coda	world-wide mb
23	760929	131	5.770	5.799	5.732	5.77
24	761020	22	5.071	5.022	4.969	4.89
25	770901	134	5.757	5.872	5.750	5.71
26	771009	27	4.845	0.000	4.637	4.51
27	780810	121	5.783	5.759	5.952	6.04
28	780927	125	0.000	5.660	0.000	5.68
29	790924	144	5.779	5.825	5.782	5.80
30	791018	120	5.737	5.664	5.821	5.85
31	801011	139	5.784	5.732	5.776	5.80
33	811001	136	5.782	5.783	5.882	5.91
34	821011	107	5.603	5.585	5.551	5.52
35	830818	105	5.807	5.739	5.769	5.84
36	830925	97	5.797	5.777	5.723	5.71
38	841025	101	5.805	5.837	5.743	5.77
39	870802	121	5.806	5.810	5.769	5.71
40	880507	97	5.719	5.654	5.614	5.52
41	881204	112	5.800	5.811	5.822	5.79
42	901024	64	5.605	5.550	5.618	5.60

Table 3.   Magnitude data from Israelsson (1992) for 17 tests at NNZ.

Event	Date	Y (kt)	mb(P)	mb(P coda)	mb(S coda)	mb(Lg)
23	760929	131	5.780	5.695	5.651	5.705
24	761020	22	5.048	5.055	5.031	4.993
25	770901	134	5.803	5.821	5.750	5.745
26	771009	27	4.788	4.819	4.698	4.735
27	780810	121	5.820	5.825	5.796	5.786
28	780927	125	5.640	5.568	5.616	5.597
29	790924	144	5.863	5.841	5.745	5.746
30	791018	120	5.813	5.756	5.725	5.720
31	801011	139	5.764	5.749	5.803	5.750
33	811001	136	5.853	5.827	5.798	5.798
34	821011	107	5.586	5.587	5.581	5.582
35	830818	105	5.792	5.779	5.813	5.824
36	830925	97	5.728	5.811	5.793	5.809
38	841025	101	5.713	5.700	5.678	5.776
39	870802	121	5.835	5.891	5.827	5.797
40	880507	97	5.644	5.690	5.716	5.714
41	881204	112	5.774	5.738	5.769	5.810

to normalize them relative to the mean NAO Lg magnitude, based on the events with magnitude between 5.603–5.807 in Table 2. Station magnitudes are assumed to be a linear combination of the network magnitude, station correction, and zero mean Gaussian error terms. Network magnitudes were obtained by solving the over-determined system of equations for the network magnitude, station correction, and standard deviation using a least squares method. The resulting network magnitudes based on the four RMS amplitudes are given in Table 3.

This set of 17 events includes all but event 42 on 24 October 1990 of the set from Ringdal and Fyen (1991). The 17 Soviet network magnitudes are based on measurements varying from three to eight stations. There were four other events analyzed by Israelsson, events 2, 4, 7, and 37, but no network magnitudes were computed for the first three because of uncertainties in the instrument characteristics at the time of these events. Network magnitudes were computed for event 37 on 26 August 1984; however, they are based on measurements from, at most, two stations and at least one of the measurements was characterized as having poor SNR. Note also that the yield for this event is represented by a dot in Figure 1, which leads to considerable uncertainty in the determined yield. Thus, we have omitted this event from the analysis below because neither the yield nor the magnitudes for this event are very reliable.

8

SECTION 3

STATISTICAL BACKGROUND

3.1 Calibration.

In this section, we present the standard linear magnitude–log yield model, for a vector of magnitude observations, and describe how the model parameters may be estimated from data. Let $\mathbf{m} = (m_1, m_2, \ldots, m_p)'$ denote the vector of p observed seismic magnitudes, where the prime superscript denotes the vector transpose, and w denote the log yield of an event. The linear magnitude–log yield regression model may then be expressed as

$$\mathbf{m} = \mathbf{a} + \mathbf{b}w + \mathbf{e}$$

$$E(\mathbf{e}) = 0 \tag{1}$$

$$Cov(\mathbf{e}) = \Sigma,$$

where the $p \times 1$ vectors, $\mathbf{a}$, $\mathbf{b}$ and $\mathbf{e}$, denote the intercept and slope parameters, and the vector of random seismic errors, respectively. We will assume that $\mathbf{e}$ has a normal distribution with zero mean and covariance matrix denoted by Σ. It is implicitly assumed in this model that the log yields are fixed observations without error.

Direct estimates of the calibration parameters, $\mathbf{a}$, $\mathbf{b}$ and Σ, may be computed if a set of measured seismic magnitudes and corresponding log yields, $\mathbf{m}_i$ and w_i (for $i = 1, \ldots, n$ events), are available from historical underground nuclear tests. For example, the vector $\mathbf{m}_i$ can represent the magnitudes based on NAO Lg, GRF Lg, NAO P coda, and world-wide m_b for the $i = 1, \ldots, 18$ events listed in Table 2. Given n previously observed values of $\mathbf{m}_i$, for which the w_i are known, unbiased estimates of $\mathbf{b}$, $\mathbf{a}$ and Σ are given by

$$\hat{\mathbf{b}} = \frac{\sum_{i=1}^{n} (\mathbf{m}_i - \overline{\mathbf{m}})(w_i - \overline{w})}{\sum_{i=1}^{n} (w_i - \overline{w})^2} \tag{2}$$

$$\hat{\mathbf{a}} \;=\; \overline{\mathbf{m}} - \hat{\mathbf{b}}\overline{w} \tag{3}$$

$$\hat{\boldsymbol{\Sigma}} \;=\; \frac{1}{n-2}\sum_{i=1}^{n}(\mathbf{m}_i - \hat{\mathbf{a}} - \hat{\mathbf{b}}w_i)(\mathbf{m}_i - \hat{\mathbf{a}} - \hat{\mathbf{b}}w_i)', \tag{4}$$

where $\overline{\mathbf{m}}$ and $\overline{w}$ are the usual sample means, given by

$$\overline{\mathbf{m}} \;=\; \frac{1}{n}\sum_{i=1}^{n}\mathbf{m}_i \tag{5}$$

$$\overline{w} \;=\; \frac{1}{n}\sum_{i=1}^{n}w_i. \tag{6}$$

(See, e.g., Fuller, 1987.) The estimates of the variances and correlation coefficients, in terms of the estimates of the covariance matrix elements, Σ_{jk}, are given by

$$\hat{\sigma}_j^2 \;=\; [\hat{\boldsymbol{\Sigma}}]_{jj}; \quad j = 1,\ldots,p \tag{7}$$

$$\hat{\rho}_{jk} \;=\; \frac{\hat{\Sigma}_{jk}}{\sqrt{\hat{\Sigma}_{jj}\hat{\Sigma}_{kk}}}; \quad j,k = 1,\ldots,p. \tag{8}$$

3.2   Yield Estimation.

Here we follow the analysis of Shumway and Der (1990) to compute a classical confidence interval for the yield of a new event. To motivate the calculation of the confidence interval, we first consider the minimum variance, unbiased estimator of the log yield

$$\hat{w} = \frac{\mathbf{b}'\boldsymbol{\Sigma}^{-1}(\mathbf{m}-\mathbf{a})}{\mathbf{b}'\boldsymbol{\Sigma}^{-1}\mathbf{b}}, \tag{9}$$

where $\mathbf{m}$ is the magnitude vector measured for the new event. Assuming that $\mathbf{m}$ has a multivariate normal distribution, a confidence interval for the log yield may be computed and a test of hypothesis that the yield is below an arbitrary threshold may

be established. Unfortunately, the calibration parameters are unknown, rendering this analysis infeasible. It is tempting to replace the unknown parameters with their estimators, $\hat{a}$, $\hat{b}$ and $\hat{\Sigma}$ in equation (9); however, the resulting distribution of the log yield estimator is not well known, and the confidence interval cannot be calculated readily.

An alternative confidence interval, considered by Shumway and Der (1990), was originally derived by Brown (1982), and has been discussed by Anderson (1984), Oman (1988) and others. Before deriving the confidence interval it is useful to express the multivariate model for n observations as

$$\mathbf{M} = \mathbf{B}'\mathbf{W} + \mathbf{E}, \tag{10}$$

where $\mathbf{M} = (\mathbf{m}_1, \ldots, \mathbf{m}_n)$ and $\mathbf{E} = (\mathbf{e}_1, \ldots, \mathbf{e}_n)$ are $p \times n$ vectors, $\mathbf{B}' = (\mathbf{a}, \mathbf{b})$ is a $p \times 2$ vector, and

$$\mathbf{W} = \begin{pmatrix} 1 & \cdots & 1 \\ w_1 & \cdots & w_n \end{pmatrix}. \tag{11}$$

The minimum variance, unbiased estimator of $\mathbf{B}$ is

$$\hat{\mathbf{B}} = \mathbf{C}^{-1}\mathbf{W}\mathbf{M}', \tag{12}$$

where

$$\mathbf{C} = \mathbf{W}\mathbf{W}' = \begin{pmatrix} n & n\overline{w} \\ n\overline{w} & \sum_i w_i^2 \end{pmatrix}. \tag{13}$$

It is straightforward to show that the expressions in (2) and (3) may be recovered from (12). Also, the unbiased estimator of Σ is given by

$$\hat{\Sigma} = (n-2)^{-1} (\mathbf{M} - \hat{\mathbf{B}}\mathbf{W})(\mathbf{M} - \hat{\mathbf{B}}\mathbf{W})'. \tag{14}$$

Using the assumptions that $\mathbf{e} \sim N(0, \Sigma)$ and that the random error vectors are independent for different events, it may be shown that $\hat{\mathbf{B}} \sim N(\mathbf{B}, \Sigma \otimes \mathbf{C}^{-1})$, i.e., has a normal distribution with mean $\mathbf{B}$ and covariance matrix $\Sigma \otimes \mathbf{C}^{-1}$, where $\otimes$ denotes the

11

Koenecker product. Using Theorems 4.3.3 and 7.2.2 of Anderson (1984, pp. 130, 249), it may also be shown that $(n - 2)\hat{\Sigma} \sim W(\Sigma, n - 2)$, i.e., has a Wishart distribution with $n - 2$ degrees of freedom.

To compute a confidence interval, note that for a new observed magnitude vector $\mathbf{m}$, associated with unknown log yield w, the multivariate residual is distributed as

$$\mathbf{m} - \hat{\mathbf{a}} - \hat{\mathbf{b}}w \sim N(0, (1 + q(w))\Sigma), \tag{15}$$

where $q(w) = (1, w)C^{-1}(1, w)'$. Now let

$$T^2 = (\mathbf{m} - \hat{\mathbf{a}} - \hat{\mathbf{b}}w)' \left[(1 + q(w))\hat{\Sigma}\right]^{-1} (\mathbf{m} - \hat{\mathbf{a}} - \hat{\mathbf{b}}w). \tag{16}$$

Using Theorem 5.2.2 of Anderson (1984, p. 163), it may be shown that

$$T^2 \frac{n - p - 1}{p(n - 2)} \sim F_{p,n-p-1}, \tag{17}$$

where $F_{p,n-p-1}$ is the F distribution with p and $n - p - 1$ degrees of freedom. (The distribution of T^2 is referred to as Hotellings T^2 distribution; T^2 is the multivariate analog of the square of a random variate t which has Student's t distribution.)

A $100(1 - \alpha)\%$ confidence interval may be obtained for the log yield w by inverting the quadratic inequality

$$T^2 \leq T^2_{p,n-2}(\alpha) = \frac{p(n - 2)}{n - p - 1} F_{p,n-p-1}(\alpha), \tag{18}$$

where $F_{p,n-p-1}(\alpha)$ is the $(1 - \alpha)$ percentile of the F distribution. Denoting the matrix elements of C^{-1} by c^{ij}, and

$$c = \hat{\mathbf{b}}'\hat{\Sigma}^{-1}\hat{\mathbf{b}} - c^{22}T^2_{p,n-2}(\alpha) \tag{19}$$

$$d = \hat{\mathbf{b}}'\hat{\Sigma}^{-1}(\mathbf{m} - \hat{\mathbf{a}}) + c^{12}T^2_{p,n-2}(\alpha) \tag{20}$$

$$e = (\mathbf{m} - \hat{\mathbf{a}})'\hat{\Sigma}^{-1}(\mathbf{m} - \hat{\mathbf{a}}) - (1 + c^{11})T^2_{p,n-2}(\alpha), \tag{21}$$

the endpoints of the interval are given by

$$\frac{d}{c} \pm \frac{\sqrt{d^2 - ce}}{c}.$$ (22)

Brown (1982) has noted that the interval may be open and is not necessarily real. Open intervals occur when the quadratic, T^2, is concave down as a function of w. The roots of the quadratic inequality for w may also be complex. These situations occur if the new magnitude information sufficiently contradicts the calibration data, or if the spread in the calibration data is too small. Examples of these pathologies will be seen in the results below.

Once the confidence interval has been computed, the midpoint of the interval is commonly used as a log yield point estimate. A yield confidence interval and point estimate may be obtained by exponentiating the log yield interval endpoints and midpoint to the tenth power. The yield and log yield point estimates are likely to be biased, i.e., $E[d/c] \neq w$ and $E[10^{d/c}] \neq y = 10^w$, in general.

A test of the hypothesis that the yield is in compliance with a treaty threshold may be established of the form: Reject the hypothesis if the lower endpoint of the confidence interval for the yield is greater than the treaty threshold. If the central value of the $100(1 - \alpha)\%$ confidence interval is unbiased, the significance level, λ, of this test would be $\alpha/2$. In general, however, the central value is a biased estimator of the yield. Thus, it can only be stated that $0 < \lambda < \alpha$. (If we had an unbiased estimate of the log yield, a strict $\alpha/2$ significance level test could be established, although it could not be expressed in closed form unless the distribution was also known. Treating the slope parameters as unknown is the fundamental cause of both complications.)

We define the F-number here such that the yield interval may be expressed as $(\hat{Y}/F, \hat{Y} \times F)$, where $\hat{Y}$ is the central value of the interval. Thus, it is given by

$$F = 10^{\sqrt{d^2 - ce}/c}.$$ (23)

Nicholson et al. (1991) also define an F-number in terms of a confidence interval. The confidence interval they derive is based on a Bayesian approach, which treats the slope and intercept parameters as unknown, while treating the covariance matrix as known.

Note that this definition is intrinsically different from the one presented by Alewine et al. (1988). The F-number given here is a random variable, while the F-number defined by Alewine et al. (1988) is a fixed quantity, defined to be the

13

value of the actual yield, such that the probability of detecting a treaty violation is 0.5, divided by the treaty yield threshold. The definition of the F-number as a fixed number, given by Alewine et al. (1988), has an appealing interpretation and, in principle, could be applied here. Unfortunately, determination of this F-number depends on the distribution of the log yield estimator and, implicitly, on the unknown slope, intercept and covariance parameters. Thus, we will adopt the definition given here and, later, estimate the mean and standard deviation of the random variable, F, by applying a jackknife procedure to the data.

3.3 Outlier Detection.

The T^2 statistic presented in the previous section can also be used to determine if a particular event in the calibration data is an outlier, i.e., to test whether the residual of an event is anomalously large. To test whether a given event is an outlier, we first perform the calibration with the remaining data to obtain estimates of the intercepts, slopes and covariance matrix. These estimates and the magnitude and log yield of the event in question are then inserted into the expression for T^2 in (16), whose value we denote by T_0^2. Since we know the distribution of T^2, we can compute the probability of obtaining a value of T^2 greater than or equal to T_0^2 and, hence, establish a test of hypothesis.

For $p = 1$ (i.e., for a one dimensional magnitude vector), T^2 is proportional to the ratio of the residual squared to the sample random error variance, and the distribution reduces to $F_{1,n-2}$. The F statistic is commonly used to test whether two samples have the same population mean. That is, in fact, what we are testing, i.e., that the population mean, μ_0, of the residual $m - \hat{a} - \hat{b}w$ for the event in question is equal to the population mean, μ, of the remaining residuals $m_i - \hat{a} - \hat{b}w_i$, $i = 1, \ldots, n-1$. As the residual $m - \hat{a} - \hat{b}w$ becomes large, the probability of obtaining a value of T^2 greater than or equal to T_0^2 becomes small. For some critical value, we reject the hypothesis that the residual of the event in question has the same population mean as the remaining sample and call the event an outlier.

More formally, let $H_0 : \mu_0 = \mu$ be the hypothesis that the population means are equal. The null hypothesis H_0 is rejected, with significance level α, if $P[T^2 \geq T_0^2] < \alpha$ or, equivalently, if $T_0^2 > T_{p,n-2}^2(\alpha)$. This test is equivalent to rejecting H_0 if the log yield of the event in question is not included in the $100(1-\alpha)\%$ confidence interval defined above. (There are other rigorous tests for outliers that could also be used, e.g., a likelihood ratio criterion.) We will apply the test given here to the data in the following sections.

14

SECTION 4

RESULTS: RINGDAL AND FYEN MAGNITUDE DATA

4.1 Calibration Results.

Using the data in Table 2, we have computed $\hat{a}_j$, $\hat{b}_j$, $\hat{\sigma}_j$, and $\hat{\rho}_{jk}$ ($j,k = 1,\ldots,4$). Since some magnitudes were not observed by all of the stations, estimates of the intercepts, slopes and standard deviations were computed using all available magnitude data recorded by the particular station, while random error correlation coefficient estimates were computed using only the intersection of events that were recorded in common by both relevant stations or networks. That is, the intercept, slope and standard deviation estimates used in the correlation estimate calculation were recomputed using only the events for which there were magnitude measurements from both stations. This correlation coefficient estimator is more robust than one that uses intercept, slope and standard deviation estimates computed from all available data.

Figure 2 shows scatter plots of the data and lines of best fit. Three lines of best fit were computed using all available data (solid), all except event 26 (dashed), and all except events 24 and 26 (dotted). Events 24 and 26 are represented by the solid square and triangle markers, respectively. The intercept, slope and standard deviation estimates are given in the legends above each frame. Random error correlation coefficient estimates, using only the events in common between relevant magnitude types are given in Tables 4–6 for these three cases. We have presented these cases to show the effect of the two small events on the slope estimates.

We have several comments regarding these results. First, NAO and GRF Lg magnitudes exhibit the least random scatter of the four sets of magnitudes. The sample random error standard deviation of NAO Lg is 0.101 for 17 events, but decreases to 0.071 when event 26 is omitted, and to 0.057 when both events 24 and 26 are omitted. For GRF Lg, the value is 0.081 for a slightly different set of 17 events, which does not include event 26. It decreases to 0.078 when event 24 is omitted. Since the standard deviations are based on slightly different sets of events, it is difficult to make a straightforward comparison. Thus, we have recomputed the results using only the 16 events that are common to all four magnitude types. Figure 3 shows scatter plots of the data and lines of best fit. The intercept, slope and standard deviation estimates are given in the legends. For this case, the sample random error standard deviation

15

Figure 2. Plots of NAO Lg, GRF Lg, NAO P coda, and world-wide m_b magnitudes versus the yields of 18 nuclear explosions at NNZ. The solid, dashed and dotted lines in each frame represent the lines of best fit using all of the available 18 events, all except event 26 (solid triangle), and all except events 26 and 24 (solid square). The parameter estimates are given in the legends above the plots.

16

Table 4. Random error correlation coefficient estimates based on the magnitude data from Ringdal and Fyen (1991).

Magnitude	NAO Lg	GRF Lg	NAO Pcoda	m_b
NAO Lg	1.000	0.787	0.844	0.771
GRF Lg		1.000	0.441	0.383
NAO Pcoda			1.000	0.968
m_b				1.000

Table 5. Correlation coefficient estimates excluding event 26.

Magnitude	NAO Lg	GRF Lg	NAO Pcoda	m_b
NAO Lg	1.000	0.787	0.664	0.557
GRF Lg		1.000	0.441	0.383
NAO Pcoda			1.000	0.946
m_b				1.000

Table 6. Correlation coefficient estimates excluding event 24 and 26.

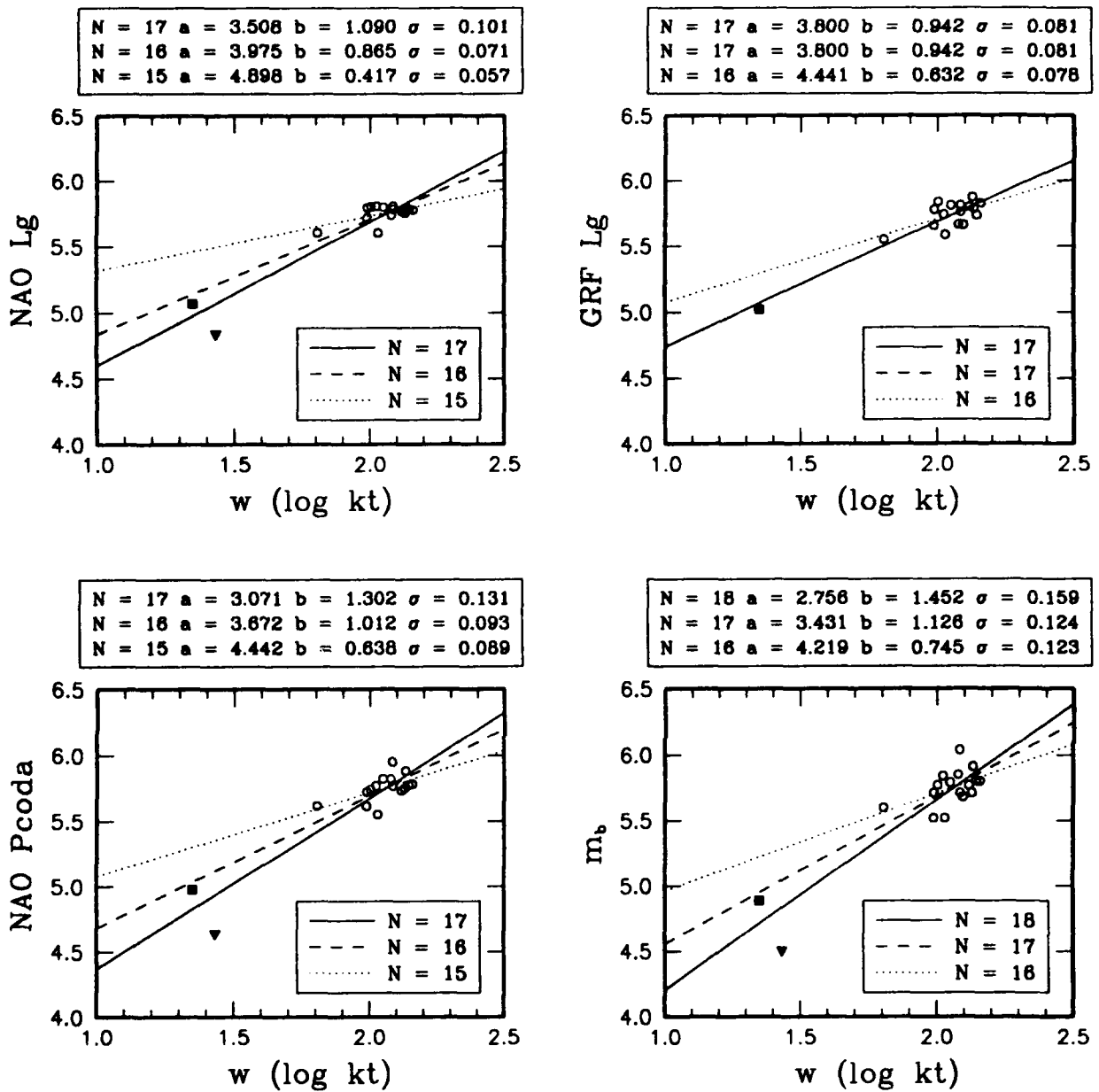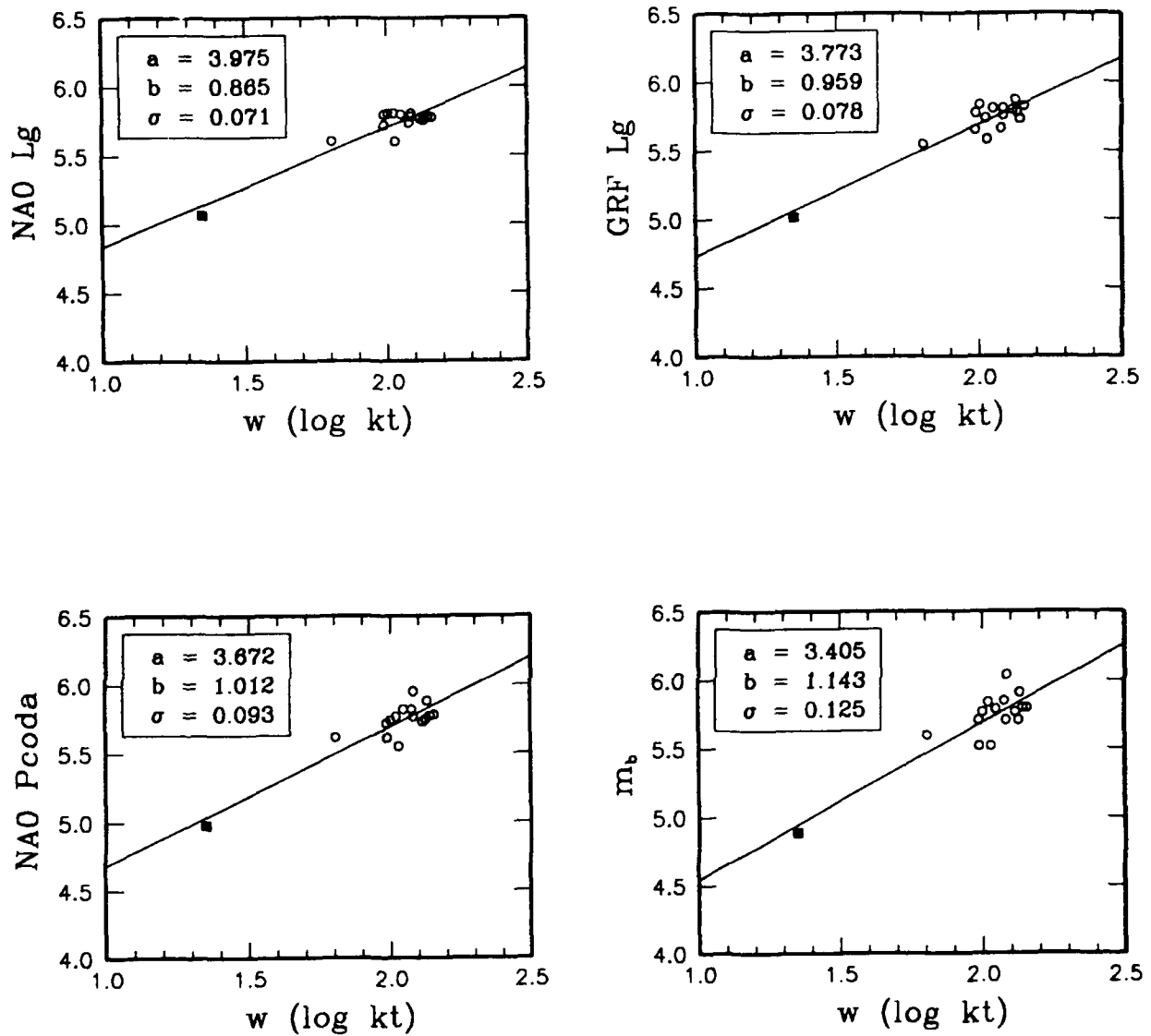| Magnitude	NAO Lg	GRF Lg	NAO Pcoda	m_b
NAO Lg	1.000	0.769	0.579	0.506
GRF Lg		1.000	0.346	0.308
NAO Pcoda			1.000	0.947
m_b				1.000

17

Figure 3. Plots of NA0 Lg, GRF Lg, NA0 P coda, and world-wide m_b magnitudes versus the yields of 16 nuclear explosions at NNZ. The same set of events are used for all four magnitude types. The parameter estimates are given in the legends above the plots.

for NA0 Lg is slightly smaller than for GRF Lg; both are smaller than those for NA0 P coda and world-wide m_b, the latter being the largest. The correlation coefficient estimates are the same as those obtained in Table 5, with the exception of the GRF Lg–m_b correlation estimate, which is 0.325 for this case.

Second, the slope estimates for the four magnitudes, based on all of the events (solid lines), are larger than expected, particularly for NA0 P coda and world-wide m_b (Figure 2). As a result, the intercept estimates are smaller than expected. Note that the slope and intercept estimates are highly dependent on the two smallest events. For example, when either event 26 or events 24 and 26 are omitted, the slope estimates decrease significantly (Figure 2). This has been referred to as the "lolly-pop" effect in regression analysis literature. Sample random error standard deviations for all four magnitudes also decrease when these events are omitted, and estimates of the NA0 Lg–NA0 P coda and NA0 Lg–m_b correlation coefficients change significantly (Tables 4–6). Since GRF Lg was not recorded for event 26, the corresponding correlation estimates only change when event 24 is also omitted and, even then, unsubstantially.

Third, the random error correlation coefficient estimates are, in some cases, remarkably high. For example, the NA0 P coda–m_b correlation estimates range from 0.946 to 0.968, depending on whether events 24 and 26 are included in the analysis (Tables 4–6). Based on all 17 events for which there were data, the NA0 Lg–NA0 P coda and NA0 Lg–m_b correlation estimates are 0.844 and 0.771, respectively. These values decrease when events 26 and 24 are omitted, but are still greater than 0.5. Similarly, the GRF Lg–NA0 Lg correlation estimate is 0.787, based on all events recorded in common, and 0.769 when event 24 is excluded. The smallest correlation estimates are obtained for GRF Lg–NA0 F coda and GRF Lg–m_b.

4.2 Outlier Analysis Results.

Significant changes in the calibration estimates when event 26, in particular, is excluded suggests that this event may be an outlier in the sense that the residuals to the lines of best fit are anomalously large. We have applied the outlier test, described in Section 3.3, successively to all of the events, and for all possible magnitude combinations, i.e., for all distinct combinations of $p = 1, 2, 3, 4$ dimensional magnitude vectors. For this analysis only the events, for which all magnitudes of the p dimensional vector were observed, were tested or included in the calibration.

Denoting the NA0 Lg, GRF Lg, NA0 P coda, and world-wide m_b magnitudes by m_1, m_2, m_3, and m_4, Table 7 lists the probabilities of obtaining values of the T^2

Table 7. Probability of $T^2 \geq T_0^2$ for events detected as outliers for all vector magnitude combinations of data from Ringdal and Fyen (1991).

Case	Magnitude Vector	Event			
		24	25	26	27
1	m_1			0.001	
2	m_2			N/A	
3	m_3			0.001	
4	m_4			0.004	
5	(m_1, m_2)	0.033	0.029	N/A	
6	(m_1, m_3)			0.003	0.039
7	(m_1, m_4)			0.004	0.032
8	(m_2, m_3)			N/A	
9	(m_2, m_4)			N/A	0.044
10	(m_3, m_4)			0.005	
11	(m_1, m_2, m_3)			N/A	
12	(m_1, m_2, m_4)			N/A	
13	(m_1, m_3, m_4)			0.011	
14	(m_2, m_3, m_4)			N/A	
15	(m_1, m_2, m_3, m_4)			N/A	

statistic greater than or equal to actual values computed, T_0^2, for events 24, 25, 26, and 27, and for all 15 possible magnitude vector combinations. These four events were the only ones with probabilities less than 0.05. Recall that T^2 is a measure of the residual of an event relative to the sample random error variance; a small probability represents a large residual, discordant with the rest of the data.

Event 24 was detected as an outlier for case 5, i.e., for the case with m = (m_1, m_2). For this case, event 24 is the only small event since m_2 was not observed. When event 24 is also removed from the calibration data, to be tested as an outlier, the lines of best fit are given by the dotted lines in Figure 2. Thus, with no other small events to influence the slope and intercept estimates, it is not surprising that event 24 was detected as an outlier. In fact, event 24 was very nearly identified as an outlier for cases 11 and 12, which also involve m_1 and m_2.

Event 25 was detected as on outlier for case 5 because the residuals contradict the calibration results. The mean magnitudes computed from the calibration data are $\overline{m}_1 = 5.710$ and $\overline{m}_2 = 5.690$, the random error standard deviation estimates are

0.072 and 0.079, and the random error correlation estimate is very high (0.876). The residuals for event 25, however, are -0.064 and +0.065, respectively, which is almost a two standard deviation difference. Furthermore, the 95% log yield confidence interval for this case is undefined, i.e., there are no real values of w for which the inequality in (18) is satisfied.

Event 27 was identified as an outlier for cases 6, 7, and 9. Cases 7 and 9 involve m_4 (world-wide m_b) for which the magnitude was 6.04, the largest of all magnitudes measured for the 18 events. Likewise, the NA0 P coda magnitude for this event was 5.952, the second largest observation for all magnitude types. Similar to event 25 for case 5, the mean calibration magnitudes are very close and the random error correlation estimates are high, but the residuals are quite different. Thus, the outliers detected for event 27 are the result of large residuals for m_3 and m_4, and the contradiction between the calibration data and this event for the different magnitude types. Note that for event 27, cases 6 and 7, there is no real value of w for which the inequality in (18) is satisfied.

Event 26 was determined to be an outlier for all cases not involving m_2 (GRF Lg). Note that m_2 was not observed for event 26. Apart from cases 5, 6, 7, and 9, event 26 was the only outlier detected. In fact, the probabilities that this event is consistent with the rest of the data are noticeably smaller than for any other event. This strongly suggests that event 26 was unusual. There are a number of possible explanations. Event 26 might have been decoupled explosion. In fact, a relatively small decoupling factor would account for the large residuals and the high slope estimates when event 26 was included in the calibration (solid lines, Figure 2). Complicated near-source topography and propagation effects could also be responsible. The actual cause of the large residuals for event 26 warrants further study.

Since event 26 has been shown to be an outlier (for whatever reason), we suggest that the best calibration estimates, based on the magnitudes from Ringdal and Fyen (1991), are those computed with event 26 excluded, i.e., the intercept, slope and standard deviation estimates corresponding to the dashed lines in Figure 2 and the correlation coefficient estimates in Table 5.

4.3 Confidence Intervals and F-Numbers.

The $100(1 - \alpha)\%$ confidence interval, presented in Section 3.2, may be used to estimate future yields, and to test compliance to the TTBT. Unfortunately, a single unified yield estimator whose distribution is known could not be obtained while

treating the slope parameters as unknown. Clearly, the large uncertainty in the slope estimates warrants this treatment. Hence, we have a confidence interval that may be applied to 15 distinct multivariate magnitude combinations. Also, since the calibration parameters are unknown, we presented a definition of the F-number which is a random variable. There are two questions we hope to answer here:

- Which multivariate magnitude combination provides the "best" confidence interval, based on the available calibration data?

- What are the means and standard deviations of the F-numbers?

To address these questions we applied jackknifing to the data. The jackknife is a resampling scheme in which each event is successively removed from the calibration data and used as a "new" event. Hence, a confidence interval and random F-number sample may be obtained for each event. Sample means and standard deviations may then be computed. In the following analysis, we set $\alpha = 0.05$.

If jackknifing is routinely applied to all of the data, several problems occur. First, the F-numbers, treating event 24 as the new one, are ill-defined for all cases involving m_2, since neither of the small events, 24 and 26, were used in the calibration. For cases 11, 12, 14, and 15, the confidence intervals are open and, hence, the sample F-numbers are infinite. For cases 2, 5, 8, and 9, the confidence intervals are closed, but the sample F-numbers are unusually large (> 200). Second, the 95% confidence interval and F-number for event 25 does not exist for case 5, nor do they exist for event 27 for cases 6 and 7; the roots of the quadratic inequality are complex. These events were identified as outliers for these cases. Third, since event 26 is an outlier for every case, none of the 95% confidence intervals include the actual yield. In fact, a 99% confidence interval would include the actual yield of event 26 in only one case (case 13). For these reasons, the results presented here were obtained by omitting event 26 from the analysis and without jackknifing on event 24, i.e., event 24 was not removed from the calibration data to be used as a new event. Also, cases with undefined confidence intervals were omitted.

Table 8 lists the F-number mean and standard deviation estimates, denoted by $\overline{F}$ and $\hat{\sigma}_F$, for all vector magnitude combinations. The third column lists the number of "new" events used to obtain the jackknife estimates. With event 26 excluded from the calibration data, the 95% confidence intervals are undefined (complex) for event 25, case 5, and event 27, case 7. The confidence intervals exist, but do not contain the actual yield for event 27, cases 4, 6, and 9 (and very nearly for case 3). These cases involve m_3 and m_4 for which the magnitudes measured for this event were

22

Table 8. Jackknife estimates of the F-number means and standard deviations for all vector magnitude combinations of data from Ringdal and Fyen (1991).

Case	Magnitude Vector	# Samples	$\overline{F}$	$\hat{\sigma}_F$
1	m_1	15	1.543	0.026
2	m_2	16	1.578	0.034
3	m_3	15	1.637	0.038
4	m_4	16	1.815	0.041
5	(m_1, m_2)	14	1.708	0.058
6	(m_1, m_3)	15	1.676	0.176
7	(m_1, m_4)	14	1.735	0.072
8	(m_2, m_3)	15	1.626	0.098
9	(m_2, m_4)	16	1.684	0.122
10	(m_3, m_4)	15	1.820	0.111
11	(m_1, m_2, m_3)	15	1.788	0.170
12	(m_1, m_2, m_4)	15	1.799	0.195
13	(m_1, m_3, m_4)	15	1.880	0.146
14	(m_2, m_3, m_4)	15	1.807	0.092
15	(m_1, m_2, m_3, m_4)	15	2.013	0.187

higher than those for events with similar yields. Last, the 95% confidence interval for event 34, case 3, does not include the actual yield. The NA0 P coda magnitude for this event is the smallest of all the events in this range.

The results in Table 8 demonstrate the following:

- Confidence intervals based on NA0 Lg magnitudes are the shortest, followed closely by those based on GRF Lg magnitudes. These magnitudes were the ones with the least random scatter.

- There is no advantage here in using intervals based on multivariate magnitude vectors. This may be a result of the high random error correlations. The lowest mean F-numbers, for a magnitude vector with $p > 1$, were obtained for cases 6, 8 and 9 for which the random error correlations are the smallest (Table 5).

- The sample F-number standard deviations for the first five cases are reasonably small, suggesting that the corresponding sample means are stable estimates.

23

SECTION 5

RESULTS: ISRAELSSON MAGNITUDE DATA

5.1 Calibration Results.

Using the Soviet network data in Table 3, we have computed calibration parameter estimates. Figure 4 shows scatter plots of the data and lines of best fit. As before, three lines of best fit were computed using all 17 events (solid), all except event 26 (dashed), and all except events 24 and 26 (dotted). Events 24 and 26 are represented by the solid square and triangle markers, respectively, and the intercept, slope and standard deviation estimates are given in the legends above each frame. Random error correlation coefficient estimates are given in Tables 9–11 for these three cases.

There are several noteworthy points regarding these results. First, the magnitudes based on RMS initial P amplitudes exhibit, surprisingly, the least random scatter with a sample random error standard deviation of 0.095, as compared to 0.111, 0.123, and 0.121 for the magnitudes based on the RMS amplitudes of P coda, S with coda, and Lg, respectively (Figure 4). Israelsson (1992) noted that there were clearly developed Lg phases at only two of the stations, APA and ARU, which were two of the three closest to NNZ. Poorly developed Lg phases at the other stations could be due to Lg blockage in the Barents and Kara Seas (Baumgardt, 1990; Israelsson, 1992). Israelsson (1992) stated, however, that there was sufficient SNR to compute RMS Lg amplitudes even for the two smallest explosions. The results obtained here suggest that Lg blockage and low SNR (relative to that of the initial P and P coda phases) may have some impact or, possibly, that near-source effects and surface interactions are responsible. Further study is needed to understand this result.

Second, the slope estimates, based on all of the events (solid lines), are again larger than expected and, hence, the intercept estimates are smaller than expected. Note that when event 26 is omitted, the slope estimates decrease significantly (Figure 4). The sample random error standard deviations also decrease for all four magnitudes when this event is omitted. When both events 26 and 24 are omitted, the slope estimates for $m_b(\text{Scoda})$ and $m_b(\text{Lg})$, in particular, are indeterminate due to the tight clustering of the remaining events. Third, the correlation coefficient estimates are remarkably high for all cases (Tables 9–11).
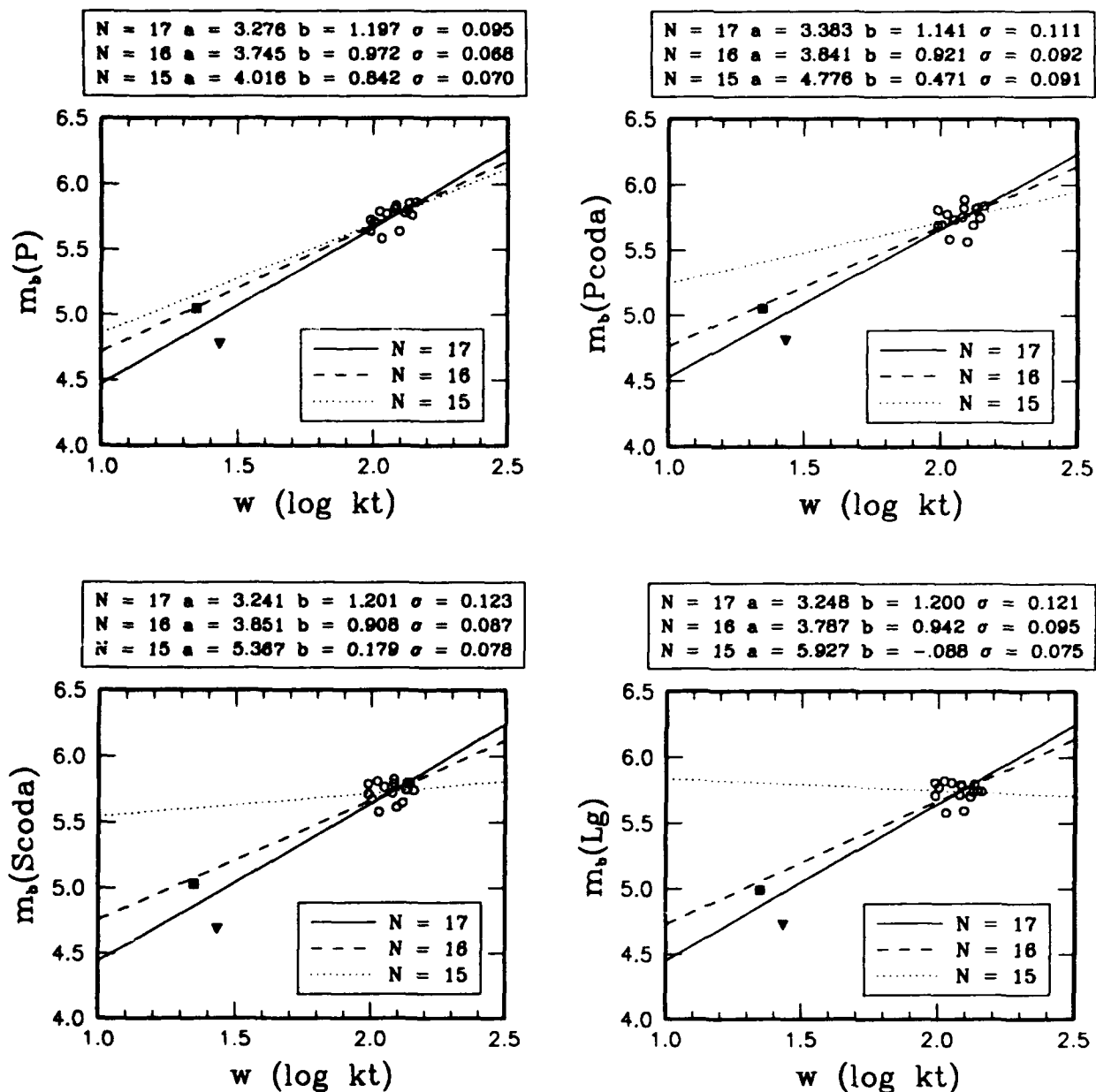
24

Figure 4. Plots of Soviet network magnitudes, based on RMS amplitutes of initial P, P coda, S with coda, and Lg, versus the yields of 17 nuclear tests at NNZ. The solid, dashed and dotted lines in each frame represent the lines of best fit using all of the available 17 events, all except event 26 (solid triangle), and all except events 26 and 24 (solid square). The parameter estimates are given in the legends above the plots.

Table 9. Random error correlation coefficient estimates for Soviet network magnitude–log yield relations, based on the magnitude data from Israelsson (1992).

Magnitude	$m_b(P)$	$m_b(Pcoda)$	$m_b(Scoda)$	$m_b(Lg)$
$m_b(P)$	1.000	0.921	0.877	0.870
$m_b(Pcoda)$		1.000	0.916	0.891
$m_b(Scoda)$			1.000	0.953
$m_b(Lg)$				1.000

Table 10. Correlation coefficient estimates excluding event 26.

Magnitude	$m_b(P)$	$m_b(Pcoda)$	$m_b(Scoda)$	$m_b(Lg)$
$m_b(P)$	1.000	0.881	0.740	0.761
$m_b(Pcoda)$		1.000	0.873	0.823
$m_b(Scoda)$			1.000	0.920
$m_b(Lg)$				1.000

Table 11. Correlation coefficient estimates excluding event 24 and 26.

Magnitude	$m_b(P)$	$m_b(Pcoda)$	$m_b(Scoda)$	$m_b(Lg)$
$m_b(P)$	1.000	0.892	0.794	0.906
$m_b(Pcoda)$		1.000	0.878	0.869
$m_b(Scoda)$			1.000	0.903
$m_b(Lg)$				1.000

Table 12. Probability of $T^2 \geq T_0^2$ for events detected as outliers for all vector magnitude combinations of data from Israelsson (1992).

Case	Magnitude Vector	Event 24	Event 26	Event 38
1	m_5	0.010	0.002	
2	m_6		0.013	
3	m_7	0.038	0.001	
4	m_8		0.006	
5	(m_5, m_6)	0.012	0.006	
6	(m_5, m_7)	0.038	0.005	
7	(m_5, m_8)	0.013	0.008	
8	(m_6, m_7)		0.005	
9	(m_6, m_8)		0.027	
10	(m_7, m_8)	0.037	0.005	0.016
11	(m_5, m_6, m_7)	0.028	0.003	
12	(m_5, m_6, m_8)	0.026	0.015	
13	(m_5, m_7, m_8)	0.011	0.010	0.047
14	(m_6, m_7, m_8)		0.014	0.047
15	(m_5, m_6, m_7, m_8)	0.005	0.005	

5.2 Outlier Analysis Results.

We have applied the outlier test, described in Section 3.3, to these data. Table 12 lists the probabilities of obtaining values of T^2 greater than or equal to the actual values computed, T_0^2, for events 24, 26, and 38, and for all distinct magnitude vector combinations. These three events were the only ones with probabilities less than 0.05. The magnitudes based on the RMS amplitudes of initial P, P coda, S with coda, and Lg are denoted by m_5, m_6, m_7, and m_8, respectively.

As in Section 4.2, event 26 is an outlier for all cases because of the large residuals. Event 24 is also an outlier for 10 of the 15 cases. This is caused by the fact that the calibration estimates are very poor when event 26 is the only small event. This also occurred for the analysis based on the magnitudes from Ringdal and Fyen (1991), but not to this degree since magnitudes for event 42 were measured. Event 42 has the third smallest yield and helped to establish reasonable slope and intercept

estimates. Soviet network magnitudes were not available for this event. If other small events were present in the data set, it is doubtful that event 24 would be an outlier.

Event 38 is an outlier for cases 10, 13, and 14, which all involve magnitudes m_7 and m_8. The mean magnitudes computed from the calibration data are $\overline{m}_7 = \overline{m}_8 = 5.632$, the random error sample standard deviations are 0.127 and 0.121, and the random error correlation estimate is 0.973. The residuals for event 38 are 0.032 and 0.131, respectively. Note that for event 38, case 10, there is no real value of w for which the inequality in (18) is satisfied.

The preceeding analysis indicates that event 26 is also unusual for this data set. Hence, we suggest that the best calibration estimates, based on the magnitudes from Israelsson (1992), are those computed with event 26 excluded, i.e., the intercept, slope and standard deviation estimates corresponding to the dashed lines in Figure 4 and the correlation coefficient estimates in Table 10.

5.3   Confidence Intervals and F-Numbers.

Here we present the jackknife estimates of the F-number means and standard deviations, based on the magnitude data from Israelsson (1992). As before, $\alpha = 0.05$, event 26 was excluded from the analysis, and the jackknife was not applied to event 24. Table 13 lists the sample F-number means and standard deviations, denoted by $\overline{F}$ and $\hat{\sigma}_F$, for all vector magnitude combinations. The third column lists the number of samples used in the jackknife procedure. The 95% confidence intervals are undefined for event 28, cases 10 and 13. The confidence intervals exist, but do not contain the actual yields for event 38, case 14, event 28, cases 1, 2, and 8, and event 34, case 1.

The results in Table 13 demonstrate the following:

- Confidence intervals based on initial P magnitudes, m_5, are the shortest, followed by those based on the $p = 2$ magnitude vectors (m_5, m_6), (m_5, m_7) and (m_5, m_8). The magnitudes based on initial P RMS amplitudes exhibit the least random scatter. The sample mean F-number for m_5 is also smaller than those based on the data from Ringdal and Fyen (1991). (Compare Tables 8 and 13.)

- There is little advantage in using intervals based on multivariate magnitude vectors. However, since the sample random error standard deviation is significantly smaller for m_5 than for the other magnitudes, the mean F-numbers for the three $p = 2$ magnitude vectors listed in item 1 are smaller than those for m_6, m_7, and m_8 individually even though the random error correlation estimates are high.

28

(Cf. the parameter estimates corresponding to the dashed lines in Figure 4 and in Table 10.)

- Most of the sample F-number standard deviations are relatively small, suggesting that the samples means are stable estimates.

Table 13. **Jackknife estimates of the F-number means and standard deviations for all vector magnitude combinations of data from Israelsson Fyen (1992).**

Case	Magnitude Vector	# Samples	$\overline{F}$	$\hat{\sigma}_F$
1	m_5	15	1.448	0.034
2	m_6	15	1.720	0.061
3	m_7	15	1.672	0.043
4	m_8	15	1.726	0.042
5	(m_5, m_6)	15	1.547	0.089
6	(m_5, m_7)	15	1.601	0.078
7	(m_5, m_8)	15	1.602	0.062
8	(m_6, m_7)	15	1.926	0.137
9	(m_6, m_8)	15	1.956	0.120
10	(m_7, m_8)	15	1.984	0.114
11	(m_5, m_6, m_7)	15	1.647	0.086
12	(m_5, m_6, m_8)	15	1.697	0.085
13	(m_5, m_7, m_8)	15	1.780	0.099
14	(m_6, m_7, m_8)	15	2.205	0.379
15	(m_5, m_6, m_7, m_8)	15	1.773	0.141

SECTION 6

CONCLUSIONS

The Soviet yield data set presented here provides the first published set of actual yields for underground nuclear tests conducted at Novaya Zemlya. We have also provided the first direct estimates of the calibration parameters for several seismic magnitudes, NORSAR Lg and P coda, Gräfenberg Lg, a world-wide m_b, and four Soviet network magnitudes, based on RMS P, P coda, S with coda, and Lg amplitudes. As noted in Sections 1 and 2.1, the accuracy of the yield data must be resolved before a high level of confidence should be placed in these results.

The calibration results in Sections 4.1 and 5.1 showed that the slope and intercept estimates depend highly on the two smallest events. In Sections 4.2 and 5.2, we showed that the residuals for one of these tests, event 26, were outliers for every relevant magnitude combination. In addition, event 26 was responsible for yielding unusually high slope and low intercept estimates. For these reasons, our best estimates of the calibration parameters are those in Tables 14–17, which were computed with event 26 excluded.

Treating all of the calibration parameters as unknown, we provided a classical 95% confidence interval, by which future yields may be estimated and compliance to a treaty threshold may be tested. An F-number was defined in terms of the interval, such that $(\hat{Y}/F, \hat{Y} \times F)$ has a 95% probability of including the actual yield, where $\hat{Y}$ is the central value of the interval. This definition was useful here because we do not have a log yield estimator whose distribution is known. Sample means and standard deviations of the F-numbers were computed for various magnitude combinations by jackknifing. The means ranged from 1.448 to 2.205 (Tables 8 and 13), depending on the magnitude combination.

Since event 26 was shown to be an outlier, there was only one small event (< 30 KT) used to estimate the slopes and intercepts; the remainder were clustered between 97 and 139 KT. Thus, the accuracy of the slope and intercept estimates depend largely on event 24. A Bayesian approach, that can incorporate *a priori* expert opinion with the magnitude–yield data, may prove to be the best method for estimating the yield of a new event and testing compliance. It provides a statistical basis for incorporating *a priori* information for cases in which the data are insufficient to compute reliable calibration estimates.

Shumway and Der (1990) have developed such an approach by which the confidence intervals may be computed analytically. Their analytic approach is somewhat limited, however, by the form of the Bayesian prior distribution for the unknown random error covariance matrix. Fisk et al. (1992) have also developed a Bayesian method which, in addition to the other information, can incorporate information available from no-yield magnitude data (irrelevant for NNZ where we actually have yield data for more events than we have magnitude data). In addition, the approach allows arbitrary specification of the Bayesian prior distribution for the covariance matrix. Yield estimates and the critical value of the hypothesis test of TTBT compliance are computed numerically. Gray et al. (1992) have extended the method of Fisk et al. (1992) to treat unknown slope parameters.

With the possibility of resumed testing at NNZ in late 1992, a simulation to assess the performances of the various yield estimation methods warrants future investigation.

31

Table 14. Best intercept, slope, and random error standard deviations estimates for NAO Lg, GRF Lg, NAO P coda and world-wide m_b magnitudes.

Magnitude	$\hat{a}$	$\hat{b}$	$\hat{\sigma}$
NAO Lg	3.975	0.865	0.071
GRF Lg	3.800	0.942	0.081
NAO Pcoda	3.672	1.012	0.093
m_b	3.431	1.126	0.124

Table 15. Best random error correlation coefficient estimates for NAO Lg, GRF Lg, NAO P coda and world-wide m_b magnitudes.

Magnitude	NAO Lg	GRF Lg	NAO Pcoda	m_b
NAO Lg	1.000	0.787	0.664	0.557
GRF Lg		1.000	0.441	0.383
NAO Pcoda			1.000	0.946
m_b				1.000

Table 16. Best intercept, slope and random error standard deviation estimates for Soviet network magnitudes based on initial P, P coda, S with coda, and Lg RMS amplitudes.

Magnitude	$\hat{a}$	$\hat{b}$	$\hat{\sigma}$
$m_b(\text{P})$	3.745	0.972	0.068
$m_b(\text{Pcoda})$	3.841	0.921	0.092
$m_b(\text{Scoda})$	3.851	0.908	0.087
$m_b(\text{Lg})$	3.787	0.942	0.095

Table 17. Best random error correlation coefficient estimates for Soviet network magnitudes based on initial P, P coda, S with coda, and Lg RMS amplitudes.

Magnitude	$m_b(\text{P})$	$m_b(\text{Pcoda})$	$m_b(\text{Scoda})$	$m_b(\text{Lg})$
$m_b(\text{P})$	1.000	0.881	0.740	0.761
$m_b(\text{Pcoda})$		1.000	0.873	0.823
$m_b(\text{Scoda})$			1.000	0.920
$m_b(\text{Lg})$				1.000

33

SECTION 7

REFERENCES

Adushkin, V., I. Kitov, V. Kovalenko, A. Peshkov, G.G. Shedlovskii, D. Sultanov (1992). Private Communication at the Fourteenth Annual PL/DARPA Seismic Research Symposium, 17-19 September 1992, Tucson, AZ.

Alewine, R.W. III, H.L. Gray, G.D. McCartor and G.L. Wilson (1988). Private Communication.

Anderson, T.W. (1984). *Multivariate Analysis*, Second Edition, John Wiley and Sons, Inc., New York.

Baumgardt, D.R. (1990). Causes of Lg Amplitude Variations and Scattering in the Eurasian Continental Crust, in Proceedings of the Twelfth Annual DARPA/GL Seismic Research Symposium, 18-20 September 1990, Key West, FL, Report GL-TR-90-0212 (Eds. J. Lewkowicz and J. Mcphetres), Phillips Laboratory, Hanscom AFB, MA. ADA226635

Brown, P.J. (1982). Multivariate Calibration, *J. R. Statist. Soc.* B **44**, 287-321.

Burger, R.W., L.J. Burdick and T. Lay (1986). Estimating the relative yields of Novaya Zemlya test by waveform intercorrelation, *Geophy. J. R. Astr. Soc.*, **87**, 523-537.

Chan, W.W., K.L. McLaughlin, R.K. Cessaro, M.E. Marshall, and A.C. Lees (1988a). Yield Estimation of Novaya Zemlya explosions from short-period body waves, Technical Report, TGAL-88-03, Teledyne Geotech, Alexandria, VA.

Chan, W.W., K.L. McLaughlin, R.-S. Jih, M.E. Marshall, and R.A. Wagner (1988b). Comprehensive magnitude yield estimation for nuclear explosions: A maximum likelihood general linear model (MLE-GLM88), Technical Report, TGAL-87-05, Teledyne Geotech, Alexandria, VA.

Fisk, M.D., H.L. Gray, G.D. McCartor and G.L. Wilson (1991), Robustness of Point Estimates for Unequal Yields, Technical Note, MRC-N-940, Mission Research Corp.

Fisk, M.D., H.L. Gray, G.D. McCartor and G.L. Wilson (1992b), A Constrained Bayesian Approach for Testing TTBT Compliance, PL-TR-91-2170, Phillips Laboratory, Hanscom AFB, MA. ADA253288

Fuller, W.A. (1987). *Measurement Error Models*, John Wiley and Sons, New York.

Gray, H.L., J. Baek, G.D. McCartor and W.A. Woodward (1992). A Bayesian Method for Testing TTBT Compliance with Unknown Intercept and Slope, SMU Technical Report.

Gray, H.L. and W.A. Woodward (1991). Yield Estimation with Unknown Intercept and Slope, Appendix in Nicholson et al. (1991).

Hurley, R.W. (1977). Anomalous seismic signals from Novaya Zemlya, AWRE Report No. O 21/77, HMSO, London, United Kingdom.

Israelsson, H. (1992). RMS Lg as a Yield Estimator in Eurasia, PL-TR-92-2117(I), Phillips Laboratory, Hanscom AFB, MA.

Jih, R.-S. and R.A. Wagner (1992). Path-Corrected Body-Wave Magnitudes and Yield Estimates of Novaya Zemlya Explosions, PL-TR-92-2042, Phillips Laboratory, Hanscom AFB, MA. ADA251240

Lay, T. (1991). Yield estimation, free-surface interactions, and tectonic release at Novaya Zemlya, in *Proceedings of the 13th Annual PL/DARPA Seismic Research Symposium*, 8-10 October 1991, Keystone, CO, Report PL-TR-91-2208 (Eds. J. Lewkowicz and J. Mcphetres), Phillips Laboratory, Hanscom AFB, MA. ADA241325

Leith, W., J.R. Matzko and J. Unger (1990). Geology and image analysis of the Soviet Nuclear Test Site at Matochkin Shar Novaya Zemlya, U.S.S.R., in *Proceedings of the Twelfth Annual DARPA/GL Seismic Research Symposium*, 18-20 September 1990, Key West, FL, Report GL-TR-90-0212 (Eds. J. Lewkowicz and J. Mcphetres), Phillips Laboratory, Hanscom AFB, MA. ADA226635

Lilwall, R.C., and P.D. Marshall (1986). Body wave magnitudes and locations of Soviet underground nuclear explosions at the Novaya Zemlya Test Site, AWRE Report No. O 17/86, MOD(PE), Blacknest, United Kingdom.

Nicholson W.L., R.W. Mensing, and H.L. Gray (1991). Private Communication.

Nuttli, O.W. (1988). Lg magnitudes and yield estimates for underground Novaya Zemlya nuclear explosions, *Bull. Seis. Soc. Am.*, **78**, 873-884.

Oman, S.D. (1988). Confidence regions in multivariate calibration, *Ann. Statist.* **16**, 174-187.

Richards, P.G. (1992). Personal Communication.

Ringdal, F. and J. Fyen (1991). RMS Lg analysis of Novaya Zemlya explosion recordings, Semiannual Technical Summary, 1 Oct 1990 - 31 Mar 1991, *NORSAR Scientific Report No. 2-90/91*, NTNF/NORSAR, Kjeller, Norway.

Russell D.R. (1990). Technical Note: Maximum Likelihood Scaling of Separate Magnitude/Yield Relationships, Headquarters, Air Force Technical Applications Center, Patrick AFB, Florida.

Shumway, R.H. and Z.A. Der (1990). Multivariate Calibration and Yield Estimation for Nuclear Tests, University of California, Davis.

Stewart, R.C., and P.D. Marshall (1988). Seismic P waves from Novaya Zemlya explosions: Seeing double!, *Geophys. J.*, **92**, 335-338.

Subhash, S.M.G., and M.A. Choudhury (1979). Coda power and modulation characteristics of a complex P signal from underground nuclear explosions, *Tectonophys.*, **53**, T33-T39.

Sykes, L.R. and S. Ruggi (1989). Soviet nuclear testing, in *Nuclear Weapon Databook* (Volume IV, Chapter 10), Natural REsources Defense Council, Washington, D.C.

Prof. Thomas Ahrens
Seismological Lab, 252-21
Division of Geological & Planetary Sciences
California Institute of Technology
Pasadena, CA 91125

Prof. Keiiti Aki
Center for Earth Sciences
University of Southern California
University Park
Los Angeles, CA 90089-0741

Prof. Shelton Alexander
Geosciences Department
403 Deike Building
The Pennsylvania State University
University Park, PA 16802

Dr. Ralph Alewine, III
DARPA/NMRO
3701 North Fairfax Drive
Arlington, VA 22203-1714

Prof. Charles B. Archambeau
CIRES
University of Colorado
Boulder, CO 80309

Dr. Thomas C. Bache, Jr.
Science Applications Int'l Corp.
10260 Campus Point Drive
San Diego, CA 92121 (2 copies)

Prof. Muawia Barazangi
Institute for the Study of the Continent
Cornell University
Ithaca, NY 14853

Dr. Jeff Barker
Department of Geological Sciences
State University of New York
 at Binghamton
Vestal, NY 13901

Dr. Douglas R. Baumgardt
ENSCO, Inc
5400 Port Royal Road
Springfield, VA 22151-2388

Dr. Susan Beck
Department of Geosciences
Building #77
University of Arizona
Tuscon, AZ 85721

Dr. T.J. Bennett
S-CUBED
A Division of Maxwell Laboratories
11800 Sunrise Valley Drive, Suite 1212
Reston, VA 22091

Dr. Robert Blandford
AFTAC/TT, Center for Seismic Studies
1300 North 17th Street
Suite 1450
Arlington, VA 22209-2308

Dr. Stephen Bratt
Center for Seismic Studies
1300 North 17th Street
Suite 1450
Arlington, VA 22209-2308

Dr. Lawrence Burdick
Woodward-Clyde Consultants
566 El Dorado Street
Pasadena, CA 91109-3245

Dr. Robert Burridge
Schlumberger-Doll Research Center
Old Quarry Road
Ridgefield, CT 06877

Dr. Jerry Carter
Center for Seismic Studies
1300 North 17th Street
Suite 1450
Arlington, VA 22209-2308

Dr. Eric Chael
Division 9241
Sandia Laboratory
Albuquerque, NM 87185

Dr. Martin Chapman
Department of Geological Sciences
Virginia Polytechnical Institute
21044 Derring Hall
Blacksburg, VA 24061

Prof. Vernon F. Cormier
Department of Geology & Geophysics
U-45, Room 207
University of Connecticut
Storrs, CT 06268

Prof. Steven Day
Department of Geological Sciences
San Diego State University
San Diego, CA 92182

1

Marvin Denny
U.S. Department of Energy
Office of Arms Control
Washington, DC 20585

Dr. Cliff Frolich
Institute of Geophysics
8701 North Mopac
Austin, TX 78759

Dr. Zoltan Der
ENSCO, Inc.
5400 Port Royal Road
Springfield, VA 22151-2388

Dr. Holly Given
IGPP, A-025
Scripps Institute of Oceanography
University of California, San Diego
La Jolla, CA 92093

Prof. Adam Dziewonski
Hoffman Laboratory, Harvard University
Dept. of Earth Atmos. & Planetary Sciences
20 Oxford Street
Cambridge, MA 02138

Dr. Jeffrey W. Given
SAIC
10260 Campus Point Drive
San Diego, CA 92121

Prof. John Ebel
Department of Geology & Geophysics
Boston College
Chestnut Hill, MA 02167

Dr. Dale Glover
Defense Intelligence Agency
ATTN: ODT-1B
Washington, DC 20301

Eric Fielding
SNEE Hall
INSTOC
Cornell University
Ithaca, NY 14853

Dr. Indra Gupta
Teledyne Geotech
314 Montgomery Street
Alexanderia, VA 22314

Dr. Mark D. Fisk
Mission Research Corporation
735 State Street
P.O. Drawer 719
Santa Barbara, CA 93102

Dan N. Hagedon
Pacific Northwest Laboratories
Battelle Boulevard
Richland, WA 99352

Prof Stanley Flatte
Applied Sciences Building
University of California, Santa Cruz
Santa Cruz, CA 95064

Dr. James Hannon
Lawrence Livermore National Laboratory
P.O. Box 808
L-205
Livermore, CA 94550

Dr. John Foley
NER-Geo Sciences
1100 Crown Colony Drive
Quincy, MA 02169

Dr. Roger Hansen
HQ AFTAC/TTR
Patrick AFB, FL 32925-6001

Prof. Donald Forsyth
Department of Geological Sciences
Brown University
Providence, RI 02912

Prof. David G. Harkrider
Seismological Laboratory
Division of Geological & Planetary Sciences
California Institute of Technology
Pasadena, CA 91125

Dr. Art Frankel
U.S. Geological Survey
922 National Center
Reston, VA 22092

Prof. Danny Harvey
CIRES
University of Colorado
Boulder, CO 80309

Prof. Donald V. Helmberger
Seismological Laboratory
Division of Geological & Planetary Sciences
California Institute of Technology
Pasadena, CA 91125

Prof. Eugene Herrin
Institute for the Study of Earth and Man
Geophysical Laboratory
Southern Methodist University
Dallas, TX 75275

Prof. Robert B. Herrmann
Department of Earth & Atmospheric Sciences
St. Louis University
St. Louis, MO 63156

Prof. Lane R. Johnson
Seismographic Station
University of California
Berkeley, CA 94720

Prof. Thomas H. Jordan
Department of Earth, Atmospheric &
  Planetary Sciences
Massachusetts Institute of Technology
Cambridge, MA 02139

Prof. Alan Kafka
Department of Geology & Geophysics
Boston College
Chestnut Hill, MA 02167

Robert C. Kemerait
ENSCO, Inc.
445 Pineda Court
Melbourne, FL 32940

Dr. Karl Koch
Institute for the Study of Earth and Man
Geophysical Laboratory
Southern Methodist University
Dallas, Tx 75275

Dr. Max Koontz
U.S. Dept. of Energy/DP 5
Forrestal Building
1000 Independence Avenue
Washington, DC 20585

Dr. Richard LaCoss
MIT Lincoln Laboratory, M-200B
P.O. Box 73
Lexington, MA 02173-0073

Dr. Fred K. Lamb
University of Illinois at Urbana-Champaign
Department of Physics
1110 West Green Street
Urbana, IL 61801

Prof. Charles A. Langston
Geosciences Department
403 Deike Building
The Pennsylvania State University
University Park, PA 16802

Jim Lawson, Chief Geophysicist
Oklahoma Geological Survey
Oklahoma Geophysical Observatory
P.O. Box 8
Leonard, OK 74043-0008

Prof. Thorne Lay
Institute of Tectonics
Earth Science Board
University of California, Santa Cruz
Santa Cruz, CA 95064

Dr. William Leith
U.S. Geological Survey
Mail Stop 928
Reston, VA 22092

Mr. James F. Lewkowicz
Phillips Laboratory/GPEH
Hanscom AFB, MA 01731-5000(2 copies)

Mr. Alfred Lieberman
ACDA/VI-OA State Department Building
Room 5726
320-21st Street, NW
Washington, DC 20451

Prof. L. Timothy Long
School of Geophysical Sciences
Georgia Institute of Technology
Atlanta, GA 30332

Dr. Randolph Martin, III
New England Research, Inc.
76 Olcott Drive
White River Junction, VT 05001

Dr. Robert Masse
Denver Federal Building
Box 25046, Mail Stop 967
Denver, CO 80225

Dr. Gary McCartor
Department of Physics
Southern Methodist University
Dallas, TX 75275

Prof. Thomas V. McEvilly
Seismographic Station
University of California
Berkeley, CA 94720

Dr. Art McGarr
U.S. Geological Survey
Mail Stop 977
U.S. Geological Survey
Menlo Park, CA 94025

Dr. Keith L. McLaughlin
S-CUBED
A Division of Maxwell Laboratory
P.O. Box 1620
La Jolla, CA 92038-1620

Stephen Miller & Dr. Alexander Florence
SRI International
333 Ravenswood Avenue
Box AF 116
Menlo Park, CA 94025-3493

Prof. Bernard Minster
IGPP, A-025
Scripps Institute of Oceanography
University of California, San Diego
La Jolla, CA 92093

Prof. Brian J. Mitchell
Department of Earth & Atmospheric Sciences
St. Louis University
St. Louis, MO 63156

Mr. Jack Murphy
S-CUBED
A Division of Maxwell Laboratory
11800 Sunrise Valley Drive, Suite 1212
Reston, VA 22091 (2 Copies)

Dr. Keith K. Nakanishi
Lawrence Livermore National Laboratory
L-025
P.O. Box 808
Livermore, CA 94550

Dr. Carl Newton
Los Alamos National Laboratory
P.O. Box 1663
Mail Stop C335, Group ESS-3
Los Alamos, NM 87545

Dr. Bao Nguyen
HQ AFTAC/TTR
Patrick AFB, FL 32925-6001

Prof. John A. Orcutt
IGPP, A-025
Scripps Institute of Oceanography
University of California, San Diego
La Jolla, CA 92093

Prof. Jeffrey Park
Kline Geology Laboratory
P.O. Box 6666
New Haven, CT 06511-8130

Dr. Howard Patton
Lawrence Livermore National Laboratory
L-025
P.O. Box 808
Livermore, CA 94550

Dr. Frank Pilotte
HQ AFTAC/TT
Patrick AFB, FL 32925-6001

Dr. Jay J. Pulli
Radix Systems, Inc.
2 Taft Court, Suite 203
Rockville, MD 20850

Dr. Robert Reinke
ATTN: FCTVTD
Field Command
Defense Nuclear Agency
Kirtland AFB, NM 87115

Prof. Paul G. Richards
Lamont-Doherty Geological Observatory
of Columbia University
Palisades, NY 10964

Mr. Wilmer Rivers
Teledyne Geotech
314 Montgomery Street
Alexandria, VA 22314

Dr. George Rothe
HQ AFTAC/TTR
Patrick AFB, FL 32925-6001

4

5

Prof. Clifford Thurber
University of Wisconsin-Madison
Department of Geology & Geophysics
1215 West Dayton Street
Madison, WS 53706

Prof. M. Nafi Toksoz
Earth Resources Lab
Massachusetts Institute of Technology
42 Carleton Street
Cambridge, MA 02142

Dr. Larry Turnbull
CIA-OSWR/NED
Washington, DC 20505

Dr. Gregory van der Vink
IRIS, Inc.
1616 North Fort Myer Drive
Suite 1440
Arlington, VA 22209

Dr. Karl Veith
EG&G
5211 Auth Road
Suite 240
Suitland, MD 20746

Prof. Terry C. Wallace
Department of Geosciences
Building #77
University of Arizona
Tuscon, AZ 85721

Dr. Thomas Weaver
Los Alamos National Laboratory
P.O. Box 1663
Mail Stop C335
Los Alamos, NM 87545

Dr. William Wortman
Mission Research Corporation
8560 Cinderbed Road
Suite 700
Newington, VA 22122

Prof. Francis T. Wu
Department of Geological Sciences
State University of New York
 at Binghamton
Vestal, NY 13901

AFTAC/CA
(STINFO)
Patrick AFB, FL 32925-6001

DARPA/PM
3701 North Fairfax Drive
Arlington, VA 22203-1714

DARPA/RMO/RETRIEVAL
3701 North Fairfax Drive
Arlington, VA 22203-1714

DARPA/RMO/SECURITY OFFICE
3701 North Fairfax Drive
Arlington, VA 22203-1714

HQ DNA
ATTN: Technical Library
Washington, DC 20305

Defense Intelligence Agency
Directorate for Scientific & Technical Intelligence
ATTN: DTIB
Washington, DC 20340-6158

Defense Technical Information Center
Cameron Station
Alexandria, VA 22314 (2 Copies)

TACTEC
Battelle Memorial Institute
505 King Avenue
Columbus, OH 43201 (Final Report)

Phillips Laboratory
ATTN: XPG
Hanscom AFB, MA 01731-5000

Phillips Laboratory
ATTN: GPE
Hanscom AFB, MA 01731-5000

Phillips Laboratory
ATTN: TSML
Hanscom AFB, MA 01731-5000

Phillips Laboratory
ATTN: SUL
Kirtland, NM 87117 (2 copies)

Dr. Svein Mykkeltveit
NTNT/NORSAR
P.O. Box 51
N-2007 Kjeller, NORWAY (3 Copies)

Dr. Michel Bouchon
I.R.I.G.M.-B.P. 68
38402 St. Martin D'Heres
Cedex, FRANCE

Prof. Keith Priestley
University of Cambridge
Bullard Labs, Dept. of Earth Sciences
Madingley Rise, Madingley Road
Cambridge CB3 OEZ, ENGLAND

Dr. Michel Campillo
Observatoire de Grenoble
I.R.I.G.M.-B.P. 53
38041 Grenoble, FRANCE

Dr. Jorg Schlittenhardt
Federal Institute for Geosciences & Nat'l Res.
Postfach 510153
D-3000 Hannover 51, GERMANY

Dr. Kin Yip Chun
Geophysics Division
Physics Department
University of Toronto
Ontario, CANADA

Dr. Johannes Schweitzer
Institute of Geophysics
Ruhr University/Bochum
P.O. Box 1102148
4360 Bochum 1, GERMANY

Prof. Hans-Peter Harjes
Institute for Geophysic
Ruhr University/Bochum
P.O. Box 102148
4630 Bochum 1, GERMANY

Prof. Eystein Husebye
NTNF/NORSAR
P.O. Box 51
N-2007 Kjeller, NORWAY

David Jepsen
Acting Head, Nuclear Monitoring Section
Bureau of Mineral Resources
Geology and Geophysics
G.P.O. Box 378, Canberra, AUSTRALIA

Ms. Eva Johannisson
Senior Research Officer
FOA
S-172 90 Sundbyberg, SWEDEN

Dr. Peter Marshall
Procurement Executive
Ministry of Defense
Blacknest, Brimpton
Reading FG7-FRS, UNITED KINGDOM

Dr. Bernard Massinon, Dr. Pierre Mechler
Societe Radiomana
27 rue Claude Bernard
75005 Paris, FRANCE (2 Copies)